

Influence of Pulsed Fiber Laser Radiation on Surface Morphology and Electrical Properties of Si/SiO₂ Structure

Dmitry Polyakov, Albert Skvortsov, Vadim Veiko

ITMO University, St.-Petersburg, Kronverkskiy pr. 49, Russia

E-mail: polyakovdmitry1988@gmail.com

The regularities of microrelief formation on the surface of Si/SiO₂ structure under the action of pulsed fiber laser radiation with intensity lower than SiO₂ damage threshold are studied. Obtained surface morphology modification accompanied with changes in capacitance-voltage characteristics of modified area.

DOI: 10.2961/jlmn.2015.03.0006

Keywords: wave-like microstructures, Si/SiO₂ structure, ytterbium fiber laser

1. Introduction

Laser microfabrication of Si and Si-based materials is a promising direction in the field of laser processing of electrotechnical materials. This trend is actual due to a potential of micro- and nano-structures development which specific properties can open perspectives for creation of new types of electronic devices. At present time there are a lot of works [1-3] devoted to laser microfabrication of silicon surface, much less attention is given to silicon – silicon dioxide structure (for example, one can see [4,5]), but it is the base for most modern microelectronic MOS devices. Since there is a big practical interest to Si/SiO₂ structure it is appropriate to use lasers which work well from the perspective of their possible use in industry. Ytterbium fiber laser is one of them. Such advantages of this laser as high efficiency, long service life, high beam quality, etc are well known. It is also possible to irradiate sample with high power nanosecond pulses (pulse energy is about 1 mJ) at high repetition rate (up to 100 kHz). This mode attracts an attention of researchers due to possible thermomechanical laser action. In particular authors have already made experiments on exposure of Si/SiO₂ structure with series of Nd:YAG-laser pulses at kilohertz repetition rate. As a result significant increase of a resistance of the SiO₂ to chemical etching was observed. However, these studies were not completed.

Let's also mention the paper [6] where specified prerequisites of possibility of obtaining nanocomposite materials (Si nanoclusters in SiO₂ layer) through direct laser irradiation of Si/SiO₂ structure were discussed. It is known that such nanostructures are promising for development of silicon-based photonic devices [7], and non-volatile memory devices [8].

For the foregoing reasons a comprehensive investigation of interaction of ytterbium fiber laser pulsed radiation with Si/SiO₂ structure is an actual scientific problem. The aim of the current work is to contribute to the solution of this problem.

In this work we studied regularities of microrelief formation on the surface of Si covered by its thermal oxide (Si/SiO₂ structure) under the action of pulsed fiber laser

radiation with intensity lower than SiO₂ damage threshold. Surface morphology of obtained microstructures was studied by methods of optical and scanning probe (AFM) microscopy. In the study of electrical properties of modified area the measuring methods of high frequency capacitance-voltage (C-V) characteristics and current-voltage (V-A) characteristics were used.

2. Experimental details

In our experiments we used monocrystalline silicon plates with crystallographic surface orientation (100) covered by thermally grown dioxide with different thicknesses (35, 150 and 500 nm) as samples. Total plate thickness was about 380 μm. Irradiation of the samples was carried out by scanning ytterbium pulsed laser beam at wavelength 1.07 μm from the oxide surface. Beam scanning was realized on the base of a biaxial galvanometer scanner - the trajectories are shown at fig. 1. Total size of irradiated area was 2×2 mm. Action of laser radiation on Si/SiO₂ structure is completely defined by following parameters: average power P, scanning speed v, pulse repetition rate f, distance between scanning lines L_y, beam diameter d and pulse duration t_p. During the exposure the beam diameter d = 120 μm and pulse duration t_p = 100 ns remained constant. Laser beam had a Gaussian profile, mentioned value of a beam diameter corresponds to e⁻² level. Parameters P, v, f, L_y were variable. We used following irradiation schemes: single pulses (v > df, L_y > d), x-axis overlapping (v << df, L_y > d), both axis overlapping (v << df, L_y << d) with one scan direction (see fig. 1a), both

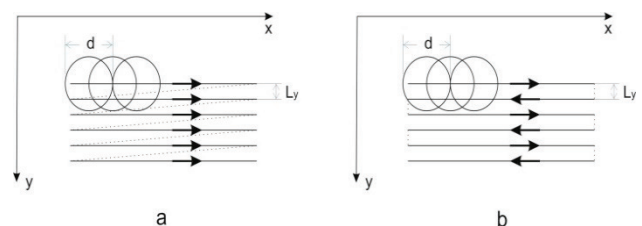


Fig.1 The beam motion pattern: a – one directional scan, b – two directional scan (scan direction shown by black arrow)

axis overlapping with changing scan direction to opposite when the beam feeds a line (see fig. 1b).

In all experiments treatment was made with intensity, which was below SiO₂ damage threshold.

3. Results

As a result of irradiation by single pulses with energy 0.17 mJ (corresponding power density $q = 1.5 \cdot 10^7 \text{ W/cm}^2$) we obtained a microrelief shown in fig. 2. It can be seen that the size of modified zone is about 30 μm (much less than beam size) regardless of SiO₂ thickness. But the style of surface morphology is significantly different for samples with different oxide thickness. Thus, in case of 500 nm dioxide thickness a tip formation occurs in the middle of irradiated zone. Such type of morphology is not found in case of thinner SiO₂ layer. The height of a tip is about 200 nm. The size of modified area and the height of a tip, as expected, increase with a growth of pulse energy.

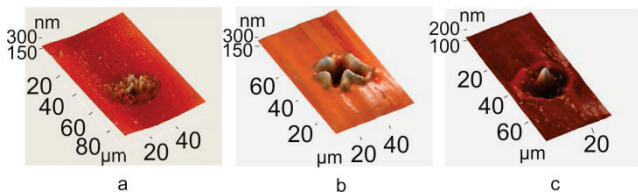


Fig.2 Microrelief, obtained after irradiation by single pulses, for samples with different oxide thickness: a – 35 nm, b – 150 nm, c – 500 nm

After irradiation of samples at x-axis overlapping mode microstructures shown in fig. 3 were observed. Processing was carried out by pulses with energy 0.13 mJ ($q = 1.15 \cdot 10^7 \text{ W/cm}^2$) on the scanning speed $v = 100 \text{ mm/s}$ at pulse repetition rate $f = 50 \text{ kHz}$. The pulse energy was reduced compared with the previous experiment, in order to avoid a destruction of an oxide film in the middle of line. The width of structured line l_0 is about 30 μm . A microrelief, obtained on samples with 35 nm oxide thickness, composed of rather chaotic cavities and protrusions. With increase of oxide thickness to 150 nm the microrelief becomes more regular and gets a herringbone structure, which is oriented in the scan direction. In case of 500 nm oxide thickness the situation is qualitatively changing. The fig. 3c shows that obtained microrelief represents a full wave period on sample's surface. Also, it can be noted that typical height of microstructures increases with increase of oxide thickness.

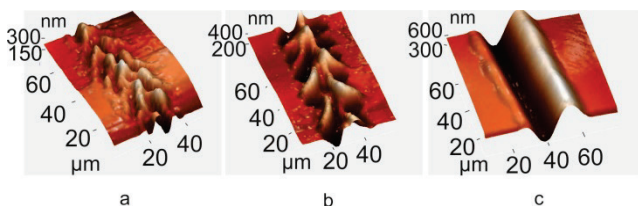


Fig.3 Microrelief, obtained in x-axis overlapping mode, for samples with different oxide thickness: a – 35 nm, b – 150 nm, c – 500 nm

The most interesting, in our opinion, results, were obtained by irradiation with both axis overlapping. Fig. 4

shows microstructures formed on Si/SiO₂ structure surface through y-axis overlapping lines ($L_y = 0.4l_0$, where l_0 is a width of single structured line), obtained in previous experiment, without scan direction changing (see fig 1a). It can be seen that in case of 150 and 500 nm oxide thickness regular plane wave-like structure is formed over the entire treated area. It is interesting that obtained structures are rotated at a certain angle to scan direction (shown by black arrow in fig. 4). Rotation of structures is observed if $L_y < 0.5l_0$. Period of waves increases with increase of oxide thickness. The period is about 15 μm for 150 nm oxide and about 36 μm for 500 nm oxide. In case of 35 nm oxide thickness the formation of wave-like structure is nearly invisible. This fact indicates an important role of SiO₂ in the formation mechanism of obtained structures. It should be noted, that orientation of wave-like structure is not related with a crystallographic orientation of samples surface.

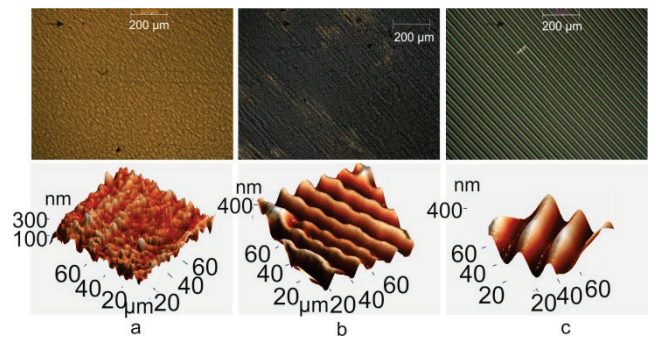


Fig.4 Microrelief, obtained in an overlapping mode along both axes without scan direction change, for samples with different oxide thickness: a – 35 nm, b – 150 nm, c – 500 nm

It was found that change of the scan direction to opposite when laser beam passes to a next line (two directional scan, see fig 1b) changes morphology style significantly. As it can be seen in fig. 5 a plane wave like structures are not observed. Microrelief gets a herringbone structure formed over the entire treated surface.

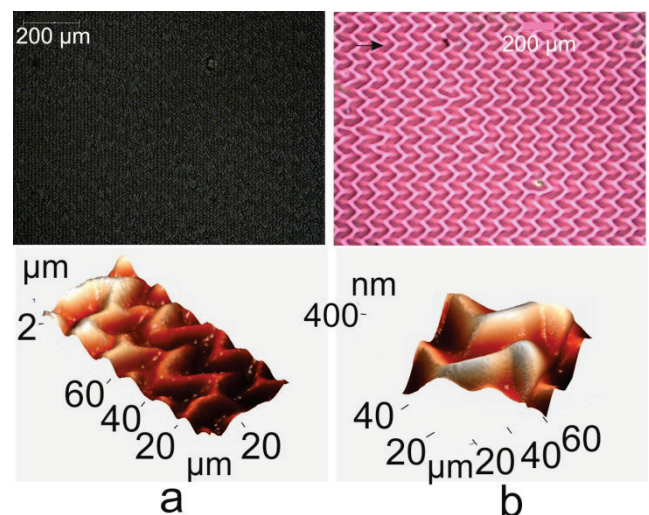


Fig.5 Microrelief, in an overlapping mode along both axes with scan direction change, for samples with different oxide thickness: a – 150 nm, b – 500 nm

To understand an influence of surface morphology on electro-physical properties capacitance-voltage (C-V) and current-voltage (V-A) characteristics were measured. For V-A characteristics measurements we used the following system of probe contacts: 4-probe contact to the back side of the plate and movable tungsten probe with micron sharpening to oxide side. For C-V characteristics measurements the tungsten probe was replaced by In-Ga contact. Fig. 6 shows typical high frequency ($\omega = 1$ MHz) C-V characteristic, normalized to the maximum value, measured on irradiated n-type silicon plate with 150 nm oxide thickness. It can be seen that there is a significant modification of C-V characteristic. Displacement of curve along the voltage axis relative to original one indicates a change of concentration of charge ΔQ_f created in SiO_2 . The change in the angle of inclination of the curve in the area of transition from inversion mode to saturation mode indicates a change in surface state density ΔN_{ss} near the interface between silicon and oxide. Capacity oscillations, which are typical for silicon nanoclusters in oxide layer, were not found.

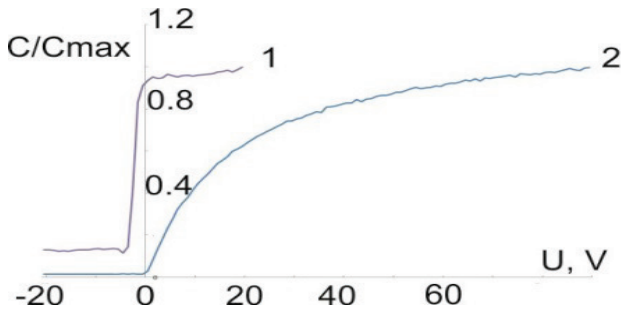


Fig 6 Typical high frequency C-V characteristic of modified area: 1 – initial sample, 2 – irradiated sample

Earlier, authors of work [9] have already drawn attention to generation of structural defects, responsible for ΔQ_f and ΔN_{ss} change in Si/SiO₂ structure under the long action (about ten seconds) of ytterbium pulsed laser radiation. In this case laser irradiation leads to plastic deformation, which is expressed in an appearance of a net of slip lines, which represents steps formed on places where dislocations rise onto a surface. In our case it is not found, and observed morphology has another nature.

Measurements of current-voltage characteristic allowed determining of breakdown voltage for laser modified area. It was found that breakdown voltage is slightly reduced (relative change is about 10 – 20%) after microstructuring. Such reduction can probably be associated with a decrease in the thickness of oxide layer. Indeed, the formation of microrelief leads to increase in surface area, resulting in decrease in SiO_2 thickness, if oxide volume is constant. Alternatively it could be an influence of an electric field increase at the maximums of the microrelief.

4. Microstructuring mechanism discussion

It is important to know typical temperatures to which sample is heated to understand the mechanism of microrelief formation. In our case it is difficult to use

standard experimental methods for temperature measuring (such as an infrared camera) due to very fast temperature oscillations. So it is advisable to use theoretical methods for temperature calculations.

In the basis of a model, which describes heating of silicon samples by series of nanosecond pulses, it is proposed to put an approach, developed in the work [10]. According to this approach it is necessary to take into account complicated dynamics of absorbed energy transfer into lattice due to nonradiative recombination of electrons excited in conduction band through interband absorption. Also, increase of an absorption by free carriers should be considered. Oxide film has not influence with a thermal physics of the process due to its small thickness and transparency. So the system of equations to be solved consists of a heat conduction equation, a free electron diffusion equation (which considers recombination) and an equation, which defines laser power density distribution inside the sample:

$$c\rho \frac{\partial T}{\partial t} - k\Delta T = S_T$$

$$\frac{\partial N}{\partial t} - D\Delta N = S_N - \frac{N}{\tau}$$

$$-\frac{\partial q}{\partial z} = (\alpha_V + \alpha_N)q$$

$$S_T = \alpha_N q + \alpha_V q \left(1 - \frac{E_g}{\hbar\omega}\right) + \frac{N}{\tau} E_g$$

$$S_N = \frac{\alpha_V q}{\hbar\omega}$$

$$\alpha_N = \sigma N$$

$$\left. \frac{\partial T}{\partial z} \right|_{z=0} = 0 \quad \left. \frac{\partial T}{\partial z} \right|_{z=H} = 0 \quad T(x \rightarrow \infty) = T(y \rightarrow \infty) = T_0$$

$$T(t=0) = T_0$$

$$\left. \frac{\partial N}{\partial z} \right|_{z=0} = 0 \quad \left. \frac{\partial N}{\partial z} \right|_{z=H} = 0 \quad N(x \rightarrow \infty) = N(y \rightarrow \infty) = 0$$

$$N(t=0) = 0$$

$$q(z=0) = (1-R)q_0$$

where $T = T(x,y,z,t)$, $N = N(x,y,z,t)$, $q = q(x,y,z,t)$ are temperature, concentration of free carriers and laser power density distribution, $c = 790$ J/(kg·K) [11] – heat capacity, $\rho = 2330$ kg/m³ [11] - density, Δ - Laplace operator, $k = 40$ W/(m·K) [11] – heat conduction coefficient, S_T – heat source, S_N – free carries source, $D = 10^{-3}$ m²/s [10] – free carriers diffusion coefficient, $\tau \sim 10^{-6}$ s [10] – characteristic time of free carriers nonradiative recombination, $\alpha_V = 2 \cdot 10^3$ m⁻¹[10] – interband absorption coefficient, α_N – free carriers absorption coefficient, $\sigma \sim 4 \cdot 10^{21}$ m² [12] – free carriers absorption cross section, $E_g = 1.1$ eV – bandgap, $R \sim 0.8$ (measured), q_0 – incident power density.

This system was solved by numerical finite-difference method.

The results of calculations are shown in fig. 7. Fig. 7a represents the temperature-time relationship of a point, situated in the middle of scanning line in the mode, in which lines shown in fig. 3 were obtained (x-axis

overlapping). This graph shows that sample haven't got enough time to cool down between pulses, and heat accumulation effect occurs. Maximal temperature is about 1950 K and it exceeds silicon melting temperature ($T_m = 1687$ K) but it is not enough for SiO_2 destruction. The width of melted area is about $28 \mu\text{m}$ (see fig. 7b). This result coincides with a width of microstructured lines, obtained in experiments ($\sim 30 \mu\text{m}$, see fig. 3). This agreement is preserved under variations of laser parameters. Fig 7c shows a comparison between widths of melted area obtained from calculations and microstructured line at different single pulse energies. On the basis of observations and calculation we can conclude, that microstructures formation is accompanied by Si melting under SiO_2 layer, which becomes soft at considered temperatures and takes the given shape easily.

The obtained structures can be hypothetically explained by a following scenario. During Si melting the Si-SiO₂ interface moves down due to decrease of Si specific volume at melted phase. So, after the melting surface looks like a concave meniscus covered by oxide. Due to radial thermal gradients a viscosity of SiO_2 in the center of melted area is smaller than at the periphery. The difference may be significant due to exponential temperature dependence of viscosity: $\eta = \eta_0 \exp(-E_\eta/R_0T)$, where η_0 – constant, $E_\eta \sim 500$ kJ/mol [13], R_0 – gas constant. According to this relation the viscosity at the periphery ($T \sim T_m = 1687$ K) should be about 50 times more than in the center of melted area ($T \sim 1900$ K). At a cooling stage the SiO_2 on the brink of melted area resists to expansion of the crystallized silicon. Thus due to a high speed of these processes an extrusion of the melt to the center and tip formation takes place (see fig. 2c). This mechanism indicates the role of SiO_2 : in case of thin oxide

layer the described effect should not be strongly demonstrated. Indeed, in case of 30 nm oxide thickness the tip formation was not observed (see fig. 2a). Described phenomena may also be accompanied by Marangoni effect as it was observed by authors [14, 15]. It can satisfactory explain the single pulse action. We believe that physical phenomena which lead to the formation of microrelief obtained in modes with spots or lines overlapping are the same. At the same time in some cases deviations from simple spot interference were obtained (for example, in the transition from fig. 2c to fig. 3c a shift of the maximum position can be seen).

In order to better appreciate all related phenomena a more complete theoretical model should include a generation of thermomechanical stresses near the interface between silicon and oxide, melting and crystallization processes, accompanied by specific volume changes, hydrodynamic features of molten silicon flow under thin oxide film etc. A detailed theoretical study of mentioned factors will reveal the most important of them and propose a complete model of microstructures formation on the surface of Si/SiO₂ structure under the action of pulsed laser radiation.

4. Conclusions

Irradiation of Si/SiO₂ structure by a scanning beam of pulsed radiation of ytterbium fiber laser leads to formation of regular wave-like structures. Its period depends on an oxide thickness. Such surface morphology modification is accompanied with changes in capacitance-voltage characteristics, which indicate a generation of structural defects responsible for creation of spatial charge and surface states in SiO_2 . A comparison between experimental data and theoretical calculations makes it possible to conclude, that surface microstructuring is accompanied by a Si melting under SiO_2 layer and its resolidification.

Acknowledgments

This work was supported by the Russian Scientific Fond Grant № 14-12-00351 (on 50%), the RFBR grant № 13-02-00033, the President of the Russian Federation Grant №. NSH 1364.2014.2 and the Government of the Russian Federation Grant №. 074-U01.

Authors thank V. Meshalkin for C-V and V-A characteristics measurements.

References

- [1] A.Y. Vorobyev, C. Guo., Appl. Surf. Sci., 257, (2011) 7291.
- [2] W.J. Mandeville, M.K. Shaffer, Y. Lu, D. O'Keefe, R.J. Knize., Appl. Phys. A, 104, (2011) 755.
- [3] Y. Han, S. Qu. Chemical Physics Letters, 495, (2010) 241.
- [4] C. T. Huynh, A. M. Skvortsov, A. A. Petrov, Proc. SPIE, 9065, (2013) 90650T-1.
- [5] C. T. Huynh, V. P. Veiko, A. M. Skvortsov, A. A. Petrov, Proc SPIE, 9065, (2013) 90650U-1.
- [6] V. P. Veiko, A. M. Skvortsov, V. I. Sokolov, Q. T. Pham, R. A. Khaletski, E. I. Efimov, Proc. SPIE, 7996, (2011) 79960S-1.

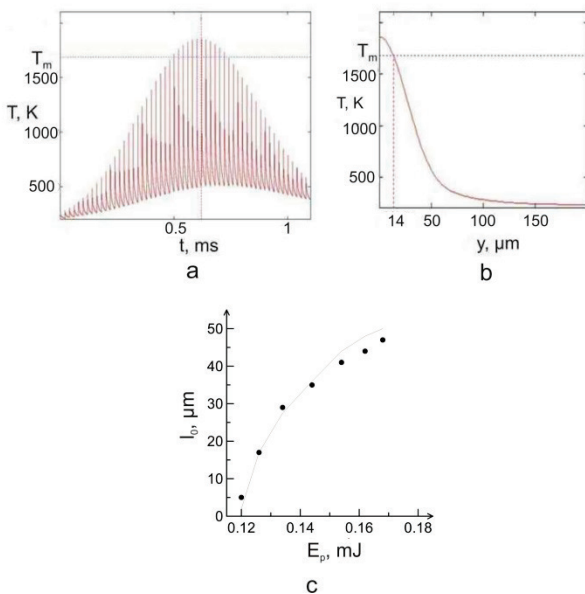


Fig.7 Results of theoretical calculations: a – temperature-time relationship of a point, situated in the middle of scanning line on a surface, b – transverse surface temperature distribution in time, when maximum temperature is achieved, c - comparison of width of melted area obtained from calculations (line) with width of microstructured line at different single pulse energies (dots, x-axis overlapping mode, $v = 100$ mm/s, $f = 50$ kHz)

- [7] S. Tivali, F. Rana, K. Chan, H. Hanafi, C. Wei, D. Buchanan, IEEE Int. Electron Devices Meeting Tech.Dig, (1995) 521.
- [8] Y. Yang, L. Xu, F. Yang, W. Liu, J. Xu, Z. Ma, K. Chen, Journal of Non-Crystalline Solids, 356, (2010) 2970.
- [9] A. Skvortsov, V. Veiko, C. T. Huynh, R. Khaletskiy, Proc. SPIE, 9065, (2013) 90650S-1.
- [10] M. Libenson: "Laser-induced optical and thermal processes in condensed medium and its reciprocal influence" ("Science", St.-Petersburg, 2007) p.423. [In Russian]
- [11] I. Grigoriev, E. Meilikhov: "Handbook of Physical Quantities" ("CRC Press", Boca Raton, 1997) p.1568
- [12] R. Dyukin, G. Martsinovskiy, G. Shandybina, E. Yakovlev, I. Nikiforov, I. Guk., Journal of Optical Technology, 78, (2011) 558.
- [13] V. Leko, O. Masurin: "Properties of Quartz Glass" ("Science", Leningrad, 1985) p. 167. [In Russian]
- [14] S. C. Chen, D. G. Cahill, C. P. Grigoropoulos, J. Heat Transfer, 122, (2000) 107.
- [15] Y. Lu, S. Theppakuttai, S. C. Chen, Appl. Phys. Lett., 82, (2003) 4143.

(Received: June 19, 2014, Accepted: June 15, 2015)